



---

## EDTA effect on Copper Sulphate Penta Hydrate- A NLO Material

R. Manimekalai<sup>1</sup> and C. Ramachandra Raja<sup>2\*</sup>

<sup>1</sup>AVVM College, Poondi, Thanjavur-613503, Tamil Nadu, India.

<sup>2</sup>Government Arts College (Autonomous), Kumbakonam – 612 001, Tamil Nadu, India.

### **Authors' contributions**

*Both the authors carried out this research work. The corresponding author CRR designed the research work. First author RM done the experimental part under the guidance of the corresponding author. The first author RM wrote the first draft of the manuscript and it was corrected and modified by the corresponding author CRR. Both authors read and approved the final manuscript.*

Research Article

Received 13<sup>th</sup> June 2013  
Accepted 20<sup>th</sup> July 2013  
Published 14<sup>th</sup> August 2013

---

### ABSTRACT

Ethylene Diamine Tetra Acetic acid (EDTA) doped copper sulphate penta hydrate were grown for five different parent-dopant combinations using slow solvent evaporation method at 300 K and good optical quality crystals were harvested for minimum dopant ratio. The single crystal X-ray diffraction studies reveal the crystal system of the doped crystal to be triclinic with cell parameters  $a = 5.963(5) \text{ \AA}$ ;  $b = 6.124(2) \text{ \AA}$ ;  $c = 10.740(2) \text{ \AA}$  and volume  $v = 365(2) \text{ \AA}^3$ ; showing that the incorporation of the dopant has not altered the structure of the parent material. The sharp well defined Bragg's peaks observed in the powder XRD pattern confirm the crystalline nature of the as grown CuEDTA complex. The powder X-ray diffraction analysis reveals the quality and purity of the grown crystal. The modes of vibrations of different molecular groups present in grown crystal were identified and the complex formation with copper was confirmed by FT-IR technique. The optical transparency with lower cut off wave length  $\sim 190 \text{ nm}$  was studied by Ultra Violet (UV)-Visible-Near IR spectral analysis. The thermal stability of the crystals was investigated by Thermo Gravimetric and Differential Thermal Analyses (TGA & DTA). The melting point of the grown crystal was confirmed by Differential Scanning Calorimetric (DSC) analysis. The endothermic peak at  $134.50^\circ\text{C}$  in DSC

---

\*Corresponding author: Email: [crraja\\_phy@yahoo.com](mailto:crraja_phy@yahoo.com);

graph indicates the melting point of the grown crystal. Vickers micro hardness study and the linear graph drawn show the mechanical properties. The surface textures like hillocks and pits were seen by chemical etching using optical microscope. The effect of the influence of dopant on the surface morphology of CuEDTA crystal faces are analyzed by scanning electron microscope (SEM). The Second Harmonic Generation (SHG) efficiency of the grown CuEDTA crystal has been tested by the Kurtz-Perry powder technique using Nd:YAG laser and was found to be 0.32 times that of KDP. The amount of EDTA ( $124 \mu\text{g/ml}$ ) present in the grown crystal was determined quantitatively by colorimetric estimation method.

*Keywords: Crystal growth; optical properties; thermal properties; X-ray diffraction; NLO material.*

## 1. INTRODUCTION

In recent years, major advances have been made in the development of nonlinear optical materials with improved optical, mechanical characteristics and damage thresholds far higher than the classical *crystals*. Many organic and inorganic materials have been identified to possess nonlinear optical property. The usefulness of a nonlinear *crystal* has been evaluated based on a set of material parameters which are directly related to the optical frequency conversion [1-4]. The ever increasing application of semiconductor based electronics creates an enormous demand for high quality semiconducting, ferroelectric, piezoelectric, oxide single crystals. Some complexes of amino acids with inorganic salts are reported to be promising materials for optical second harmonic generation [5]. The dopant EDTA is also known as artificial amino acid and it is a hexa dentate ligand. It binds through the four oxygens and two nitrogens to the central metal copper ion [6]. The effect of impurities on growth rates and morphology have been discussed in many articles [7-12], hence we have grown the non-linear optical ethylene diamine tetra acetic acid doped copper sulphate penta hydrate single crystals. As no reports are available on the growth and characterization of EDTA doped copper sulphate penta hydrate single crystals, in this work, we report on the growth and characterization of EDTA doped copper sulphate penta hydrate (CuEDTA) crystals by slow evaporation technique.

## 2. EXPERIMENTAL

The saturated solutions of copper sulphate penta hydrate at 300 K were prepared with the series of compositions varying from 1 to 5 mole percent ethylene diamine tetra acetic acid at pH 5 were used to grow CuEDTA single crystals. Thus prepared solutions were stirred thoroughly for 5-6 hours. Finally, the solution was filtered using filter paper (Whatman no.450) and tightly closed for controlled evaporation of the solvent. Crystals from all the compositions were allowed to grow for 7-10 days from the time of nucleation. Good quality and transparent single crystals with minimum dopant ratio of dimensions  $3.4 \times 1.5 \times 0.5 \text{ cm}^3$  were harvested and are shown in the Fig. 1. Under high acidity growth rate decreases considerably and there may be a chance to form slightly soluble copper hydroxides [13,14].

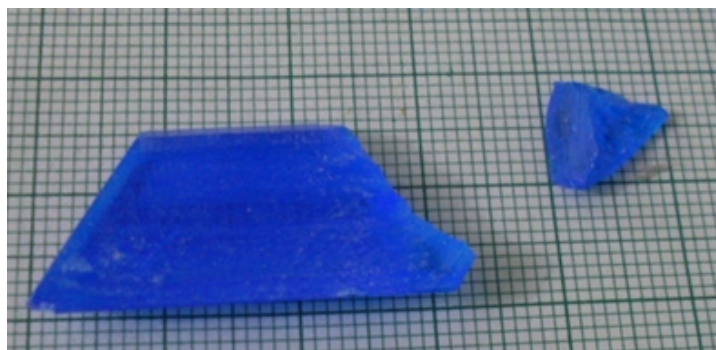


Fig. 1. As grown CuEDTA crystals

### 3. RESULTS AND DISCUSSION

#### 3.1 X-ray Diffraction Studies

Jeffery GH et al reported the structure of the CuEDTA. EDTA binds through the four oxygens and two nitrogens to the central metal copper ion [6] and its structure is as shown in Fig. 2.

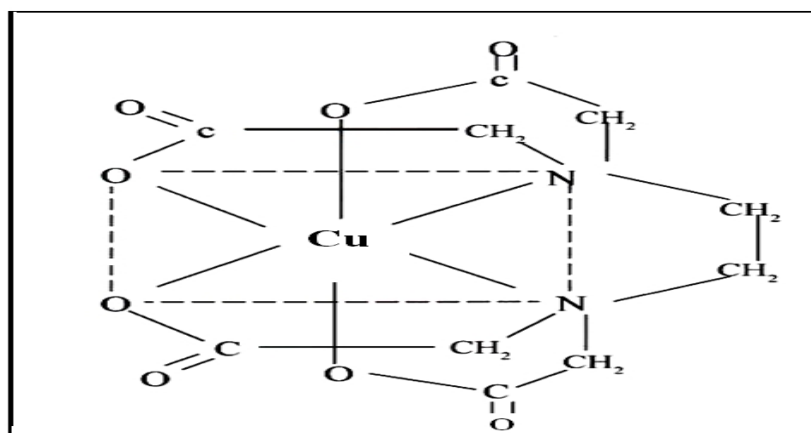


Fig. 2. Structure of CuEDTA

The single crystal XRD of the grown CuEDTA crystals were recorded using BRUKER NONIUS CAD4 single crystal x-ray diffractometer with Cu  $K_{\alpha}$  radiation ( $\lambda=1.5405 \text{ \AA}$ ). Single crystal XRD report confirms the grown CuEDTA crystal belongs to the triclinic system with the lattice parameters  $a = 5.963(5) \text{ \AA}$ ;  $b = 6.124(2) \text{ \AA}$ ;  $c = 10.740(2) \text{ \AA}$ , volume  $v = 365(2) \text{ \AA}^3$ ;  $\alpha=77.08(3)^{\circ}$ ;  $\beta = 82.62(1)^{\circ}$  and  $\gamma=73.03(1)^{\circ}$ . Powder XRD analysis has been carried out using Rich – Seifert powder diffractometer with  $\lambda=1.54 \text{ \AA}$  to confirm the crystalline nature and also to ascertain the purity of the grown CuEDTA crystal as shown in Fig. 3. The diffraction planes are indexed with the help of the computer program, TJB Holland and SATRED FERN 1995 as shown in Fig. 3. The lattice parameters from both powder XRD, single crystal XRD of the grown crystal and also unit cell dimension of pure  $\text{CuSO}_4 \cdot 5\text{H}_2\text{O}$  are shown in Table 1.

The observed  $2\theta$ ,  $d$  and  $hkl$  indices of the corresponding reflecting planes are shown in Table 2.

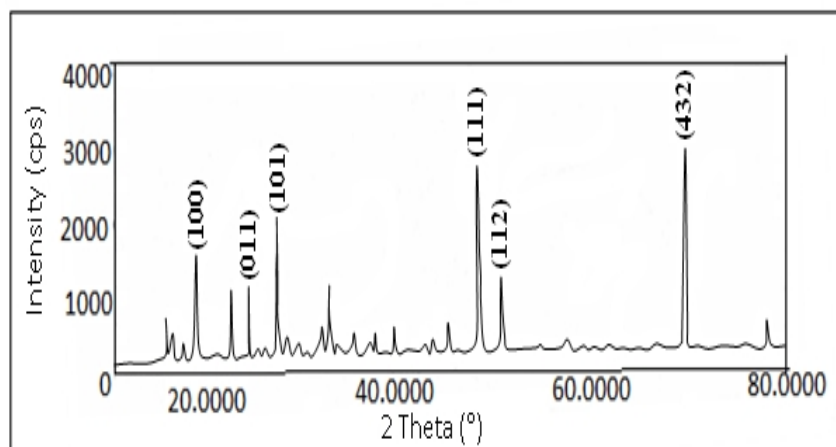


Fig. 3 Powder XRD pattern of CuEDTA

Table 1. Lattice parameters of CuEDTA and Copper sulphate penta hydrate

CuEDTA	CuSO <sub>4</sub> .5H <sub>2</sub> O
<b>Powder XRD</b>	<b>Single crystal XRD</b>
a=5.9866 Å	a=5.963(5) Å
b=6.1321 Å	b=6.124(2) Å
c=10.7715 Å	c=10.740(3) Å
v=368.24 Å <sup>3</sup>	v= 365(2) Å <sup>3</sup>
Structure : Triclinic	Structure :Triclinic
$\alpha=77.10^0$	$\alpha=77.08(3)^0$
$\beta=83.09^0$	$\beta=83.51(3)^0$
$\gamma=73.14^0$	$\gamma=73.03(1)^0$
	a=5.953(4) Å
	b=6.088(4) Å
	c=10.670(6) Å
	v=359.6(4) Å <sup>3</sup>
	Structure : Triclinic
	$\alpha=102.57(6)^0$
	$\beta=97.50(5)^0$
	$\gamma=107.28(8)^0$

Table 2. X-ray powder data of CuEDTA

$2\theta^0$	d (Å)	hkl
15.580	5.6829	100
16.140	5.4870	011
16.320	5.4269	001
17.140	5.1691	002
17.360	5.1040	101
18.900	4.6915	111
22.360	3.9727	112
24.160	3.6807	1 10
27.120	3.2853	1 12
32.640	2.7412	0 13
47.860	1.8990	2 13
47.980	1.8946	300
69.080	1.3586	414
69.280	1.3551	432

### 3.2 FTIR Spectral Analysis

The Fourier transform infrared spectral analysis is a technique in which almost all functional groups in a molecule absorb characteristic frequencies. The FTIR spectrum was recorded in the range 400-4000  $\text{cm}^{-1}$ , by Perkin-Elmer spectrometer (KBr pellet technique). The FTIR spectrum of pure EDTA, CuEDTA and  $\text{CuSO}_4 \cdot 5\text{H}_2\text{O}$  is shown in Figs. 4a, 4b and 4c respectively. A close observation of FT-IR spectra of the parent and CuEDTA show the doping results in small shifts in some of the characteristic vibrational frequencies. It is seen from the spectra that CuEDTA spectrum is having more or less the same peaks with slightly different frequencies. The C=O stretching frequency of carboxyl group appear at 1624  $\text{cm}^{-1}$  in EDTA is shifted to 1632  $\text{cm}^{-1}$  of CuEDTA. This indicates that EDTA has coordinated to the  $\text{Cu}^{2+}$  ions [15-17]. The peaks appearing nearly at 1463  $\text{cm}^{-1}$  for the pure sample and that at 1460  $\text{cm}^{-1}$  for the grown sample are due to  $\text{SO}_4$  symmetric stretching. The N-H stretching frequency occurs at 3530  $\text{cm}^{-1}$ . The peak at 621 and 618  $\text{cm}^{-1}$  may be representing  $\text{SO}_4$  of parent and the grown crystal. The characteristic frequency at 1143  $\text{cm}^{-1}$  for Cu (II) complex of the grown crystal, which is not present in the parent, is confirming the efficient formation of the stable complex. The comparison and functional group assignment of IR bands of CuEDTA with pure EDTA and  $\text{CuSO}_4 \cdot 5\text{H}_2\text{O}$  are shown in the Table 3.

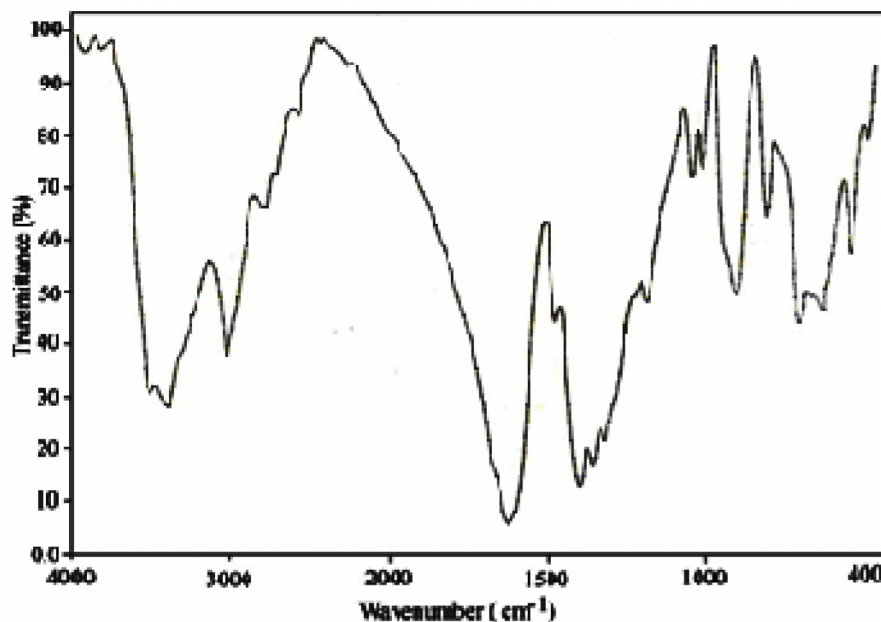


Fig. 4a. FT-IR spectrum of pure EDTA

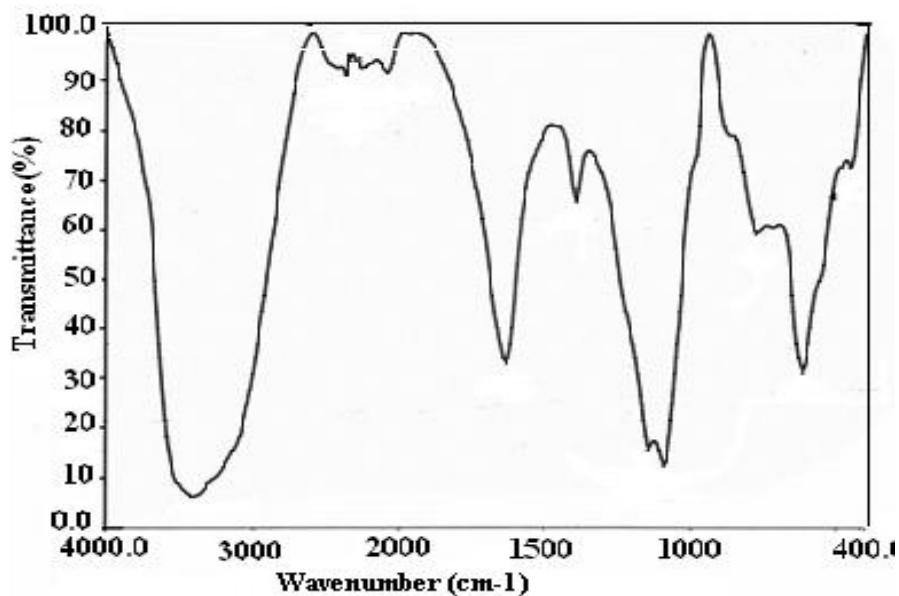


Fig. 4b. FT-IR spectrum of CuEDTA

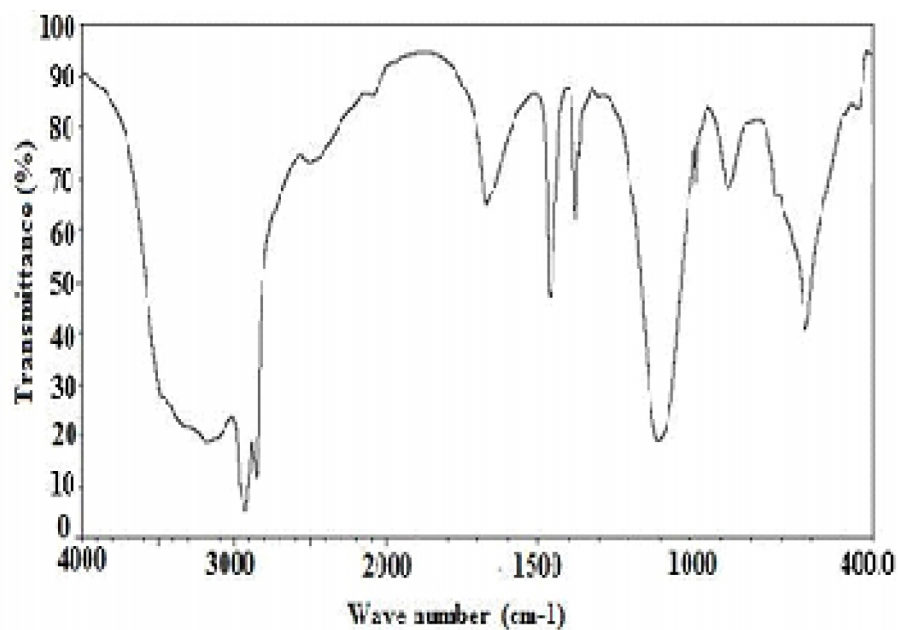


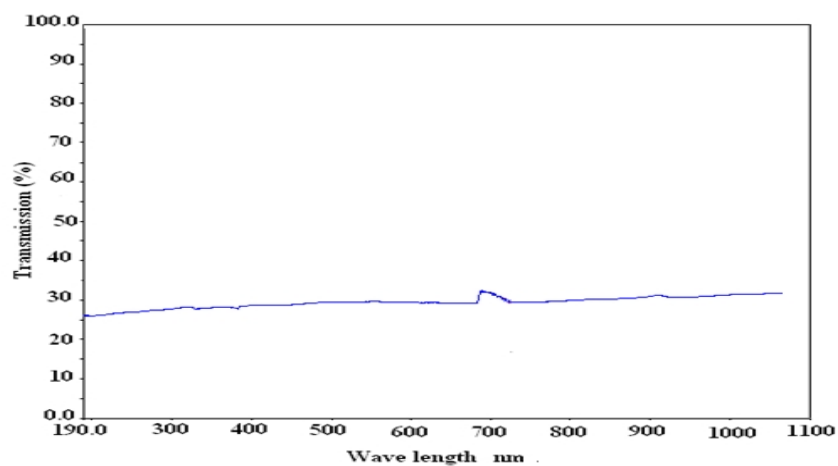
Fig. 4c. FT-IR Spectrum of pure Copper Sulphate Penta Hydrate

**Table 3. Comparison of IR bands of CuEDTA with pure EDTA and ETGS in  $\text{cm}^{-1}$** 

CuSO <sub>4</sub> .5H <sub>2</sub> O ( $\text{cm}^{-1}$ )	CuEDTA ( $\text{cm}^{-1}$ )	EDTA ( $\text{cm}^{-1}$ )	Tentative frequency assignment
---	3530	3516	N-H stretching
2966	---	---	H <sub>2</sub> O bending
2926	---	---	H <sub>2</sub> O stretching
2655	---	---	H <sub>2</sub> O rocking
1671	---	---	H <sub>2</sub> O asym.stretching
---	1632	1624	C=O stretching of carboxylate ion
1463	1460	---	SO <sub>4</sub> symmetric stretching
1377	1394	---	SO <sub>4</sub> asym. stretching
---	1325	1319	C-N sym.stretching
---	1143	1120	C-H stretching
1106	1091	---	O-H bending
982	774	---	SO <sub>4</sub> -non-degenerate mode
621	618	---	SO <sub>4</sub> - degenerate mode
451	434	---	N-C-N stretching

### 3.3 UV-VIS- NIR Spectral Analysis

The UV-Vis-NIR transmission spectrum of the grown crystal were recorded in solution state between 190 and 1100 nm using Lamda 35 UV-Vis-NIR spectrophotometer. The recorded UV- Vis-NIR transmission spectrum of the grown CuEDTA crystal is shown in the Fig. 5. From the spectrum, it is noted that the UV transparency cut off is  $\sim 190\text{nm}$  and there are no significant absorptions observed in the entire region of the spectrum. The transmission extends nearly from 200nm to 1100nm, makes it valuable for those applications requiring blue/green light. It is an important requirement for NLO materials having nonlinear optical applications [18,19].

**Fig. 5. Transmission spectrum of CuEDTA**

### 3.4 Micro Hardness Study

Mechanical strength of CuEDTA crystal was studied by measuring micro hardness and it plays an important role in the fabrication of opto-electronic devices. The hardness of a material is a measure of its resistance to plastic deformation. The permanent deformation can be achieved by indentation, bending, scratching or cutting [20]. The values of micro hardness number at different loads applied to the sample is provided in the Table 4 and it is noticed that Vickers hardness number ( $H_v$ ) increases with the applied load as shown in Fig. 6.

**Table 4. Variation of hardness value with load**

Load in grams	Hardness value in kg/mm <sup>2</sup>
25	29.1
50	36.3
100	44.3
200	69.15

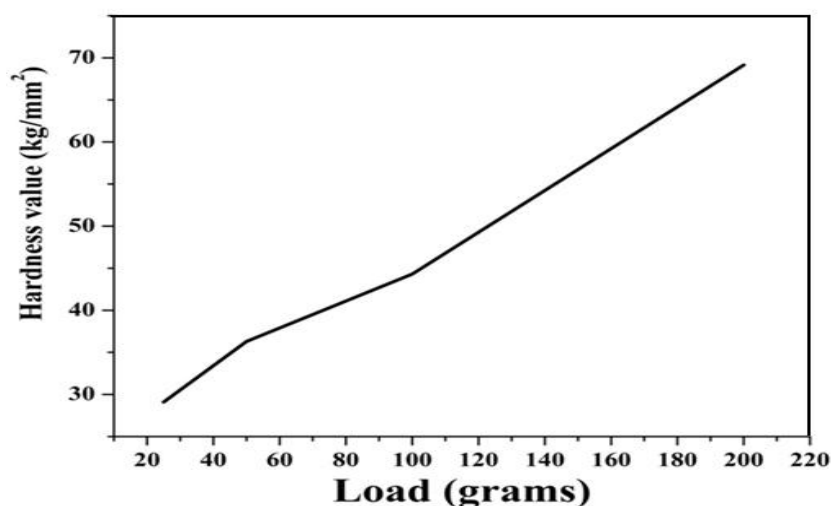


**Fig. 6. Variation of hardness value with load**

### 3.5 Colorimetric Estimation Method

Unknown compounds may be identified by their characteristic absorption spectra in the ultraviolet, visible or infrared regions. Color reactions frequently can be followed by measuring spectrophotometrically the appearance of permanent colour (pale pink) of the product. A spectrophotometer /colorimeter is an instrument for measuring the absorbance of a solution by measuring the amount of light (optical density) of a given wavelength that is transmitted by a sample. Ninhydrin will react with amino group,  $\text{NH}_2\text{-C-COOH}$ , called auxochromes. The ninhydrin reaction, one of the most important methods of detecting amino acids, both technically and historically, has been conventionally used to detect their microgram amounts. To determine the absolute concentration of a pure substance, a standard curve is constructed from the known concentrations and using that standard curve, the absorbance reading (optical density) of the sample concentration was determined. The



colour intensity (optical density-0.037) was measured by deep vision colorimeter (digital) at 540 nm [21,22]. The amount of EDTA present in our crystal was found to be 124  $\mu$  gram/ml which is less than the amount of EDTA (1.989 mg/ml) present in the solution.

### 3.6 Thermal Analysis

Thermo gravimetric analysis (TGA), differential thermal analysis (DTA) and differential scanning calorimetric technique (DSC) were carried out using SDT Q600 V20.5 Build15 analyser in nitrogen atmosphere at a heating rate of 20°C /min and were recorded in the same chart as shown in Fig. 7. The weight of the sample taken for investigation was 10.56202 mg. The weight loss was observed in two steps. In the first step, the weight loss starts at 87.50°C and completes ~at 110°C. It may be due to the elimination of two water molecules. At this stage, the sample may be emerged as trihydrous salt. Around 134.50°C, it is in the molten state and at this temperature the third water molecule may be liberated. At the temperature ~134.50°C, there is one endothermic peak in DSC graph which corresponds to the melting point of the grown crystal. On further heating, again the second weight loss occurs. Hence at temperatures ~220°C and 268°C the other remaining water molecules are liberated. This is confirmed by the two endothermic peaks that are occurring in DSC. At these temperatures the remaining two water molecules are liberated and then the sample is remaining as an anhydrous salt. Beyond 268°C, all the hexa dentate ligands are eliminated and CuSO<sub>4</sub> is reduced to CuOH [23-24].

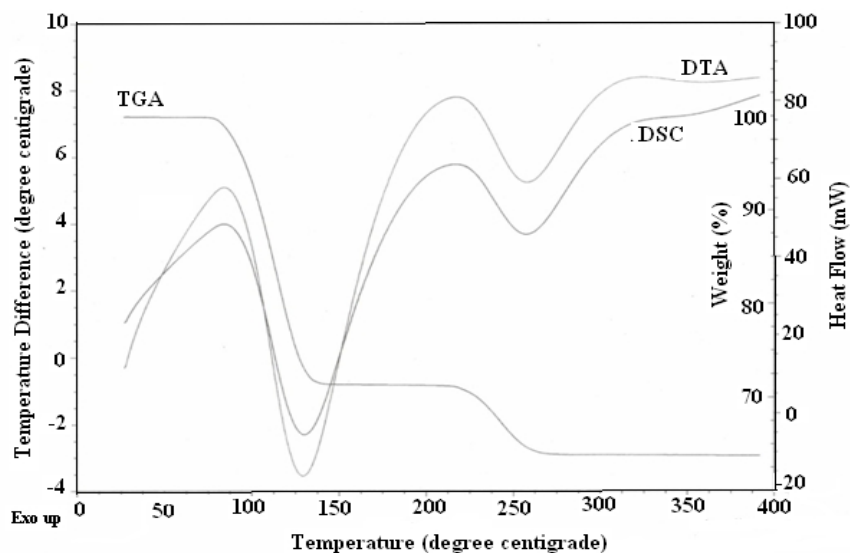
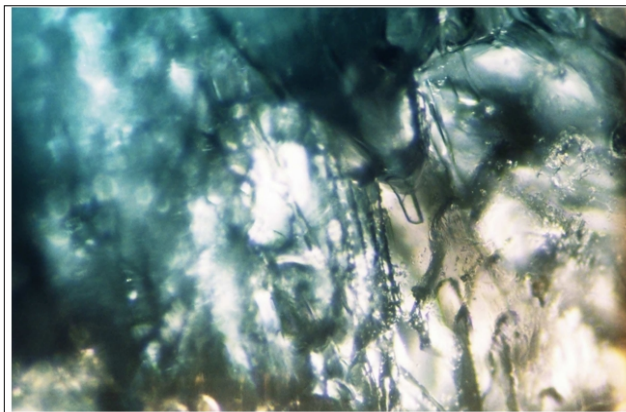


Fig. 7. TGA, DTA and DSC of CuEDTA

### 3.7 Etching Study

The defects present in the grown crystals can be analyzed by a simple technique known as chemical etching. Once the damaged surface layer is removed by means of etching, a fresh surface appears which in turn gives clear pits. The etched surface is dried and examined. The grown crystal before etching (Fig. 8a) was examined through the optical microscope, Leitz Metallux-II. The crystal was etched by 0.5M ethanol etchant for five seconds and then

analyzed through the same microscope. Some well defined crystallographically aligned etch pits, valleys, hillocks and some islands were observed on the surface as shown in Fig. 8b.



**Fig. 8a. Etch pattern-before etching**

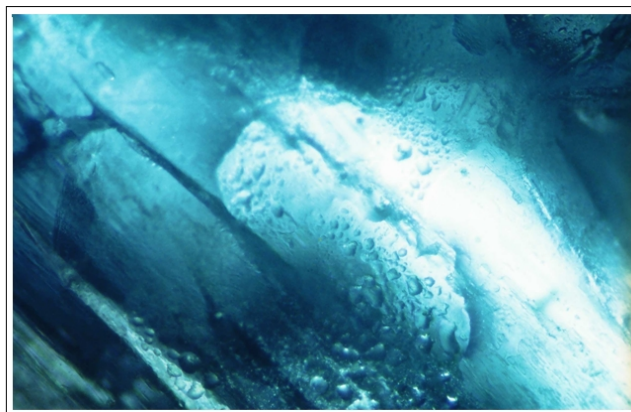


**Fig. 8b. Etch pattern-after etching**

### **3.8 Scanning Electron Microscope Analysis**

Scanning the surface with a high energy beam of electrons in a raster scan pattern is called Electron microscope. The shape and size of the particles making up the object can be viewed and studied. The HITACHI-S-3000H instrument is used to examine surface morphology of the grown crystal. Figs. 9(a, b, c, d) show the SEM images of the as grown CuEDTA crystal. The SEM micrographs show the purity and crystalline nature of the grown crystals. It is seen from the SEM pictures that the surface of the as grown crystal is smooth and consist of uniformly dispersed clusters [25]. It is also seen that there are more coalescence of particles, agglomerating into distinct islands. These islands eventually coalesce to form a continuous lattice.

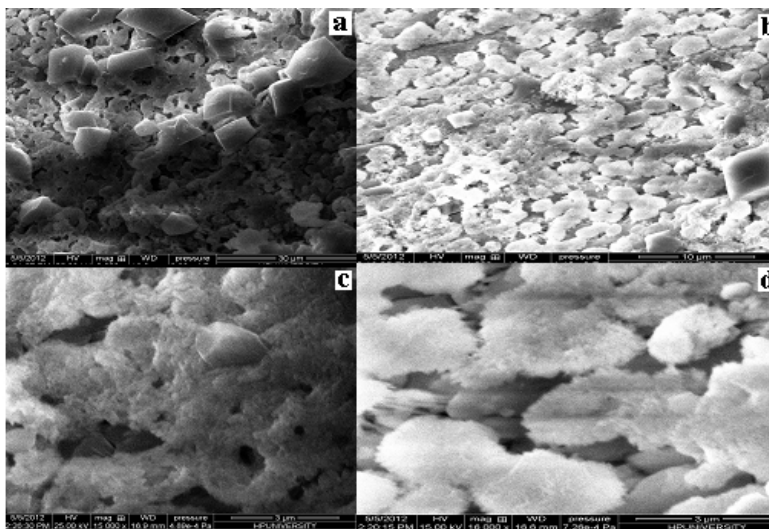


Fig. 9. (a, b, c, d) SEM micrographs of CuEDTA

### 3.9 Second Harmonic Generation Test

Second harmonic generation from powder CuEDTA crystal with reference to KDP was studied by following the technique developed by Kurtz and Perry [26]. The schematic diagram of this method is shown in the Fig. 10. The presence of delocalized  $\pi$  electron systems is the microscopic origin of dielectric polarizability [27]. In this experiment, Q-switched Nd-YAG laser with the first harmonic output of 1064 nm was used. The crystal was ground to homogeneous powder and tightly packed in a micro capillary tube and mounted in the path of the laser beam of pulse energy 0.68 mJ. The SHG was confirmed by the emission of green light ( $\lambda=532$  nm) collected by photo multiplier tube and displayed on the oscilloscope. SHG signals of intensity 2.8 mV were recorded for the CuEDTA sample. The second harmonic generation efficiency of CuEDTA is 0.32 times that of KDP.

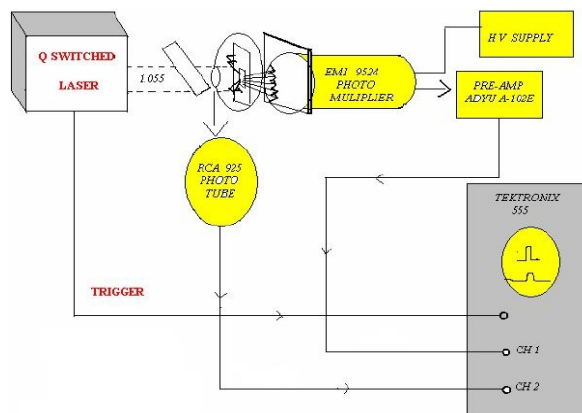


Fig. 10. Schematic diagram of SHG test

#### **4. CONCLUSION**

CuEDTA crystals were grown using water as the solvent at ambient temperature. The slow evaporation of the solvent yielded good quality crystals. The lattice parameter values were determined by single crystal XRD and the crystalline nature of grown crystal had been confirmed by powder XRD. The presence of various functional groups was identified by FTIR analysis. The UV-Visible spectrum reveals that the grown crystals are transparent in the wavelength region 200-1100nm. Thermal analyses revealed that the grown crystals are thermally stable up to 135°C. The DSC analysis shows the presence of endothermic phase transitions at 135°C, 220°C and 268°C. The peak observed at 135°C in the DSC corresponds to the melting point of the material. The Vickers micro hardness test was carried out to understand the mechanical properties. The surface morphology is understood by etching studies. The presence of the dopant was confirmed by colorimetric estimation method. The concentration of EDTA in the grown crystal was 124 µg/ml. The second harmonic generation property of the grown crystal was confirmed by the emission of green light.

#### **COMPETING INTERESTS**

Authors have declared that no competing interests exist.

#### **REFERENCES**

1. Dmitriev VG, Gurzdyan GG, Nikogosyan DN. Hand Book of Nonlinear Optical Crystals. Springer- Verlag, New York; 1999.
2. Muthu K, Meenakashisundaram SP. Growth and characterization of Hexakis (thiourea) nickel (II) nitrate crystals. *J. Cryst. Growth*. 2012;352:158-162.
3. Ramachandra Raja.C, Sundararajan RS, Krishnakumar V. FT-IR, FT-Raman and thermal studies of bistiourea manganese Chloride – An organo metallic crystal. *Spectrochimica Acta A*. 2009;71:1634-1637.
4. Dhumane NR, Hussaini SS, Dongre VG, Mahendra D. Shirsat. Influence of glycine on the nonlinear optical (NLO) properties of zinc (tris) thiourea sulfate (ZTS) single crystal. *Optical Material*. 2009;31:328-332.
5. Chandrasekaran J, Illayabarathi P, Maadeswaran P, Mohamed Kutty P, Pari S. Synthesis, growth and characterization of a semiorganic nonlinear optical single crystal: L-Valine cadmium bromide. *Optik*. 2012;123:1407-1409.
6. Jeffery GH, Bassett J, Mendham J, Denney RC. Vogel's text book of Quantitative chemical Analysis (ELIBS). Addison Wesley Longman Limited. UK; 1989.
7. Meera K, Claude A, Muralidharan R, Choi CK, Ramasamy P. Growth and characterisation of EDTA-added TGS crystals. *J. Cryst. Growth*. 2005;285:358-364.
8. Lawrence M, Thomas Joseph Prakash. Growth and characterization of pure and glycine doped cadmium thiourea sulphate (GCTS) crystals. *Spectrochimica Acta Part A*. 2012;91:30-34.
9. Muthu K, Meenakashisundaram SP. Synthesis, growth, structure and characterization of a new semiorganic crystal: Tetrakis(thiourea)zinc(II) picrate. *Materials Letters*. 2012;84:56-58.
10. Ramachandra raja C, Ramamurthi K, Manimekalai R. Growth and spectral characterization of ethylene diamine tetra acetic acid (EDTA) doped zinc sulphate hepta hydrate - A semi organic NLO material. *Spectrochimica Acta: Part A*. 2012;99:23-26.

11. Ramachandra raja C, Vijayabhaskaran B. Synthesis, growth and characterization of a new nonlinear optical crystals copper cobalt thiocyanate. Indian Journal of Pure and Applied Physics. 2011;49:531-534.
12. Vijayabhaskaran B, Arivazhagan, Ramachandra raja C. Synthesis, growth and characterization of copper mercury thiocyanate crystals. Indian Journal of Pure and Applied Physics. 2011;49:340-343
13. Dongli Xu, Dongfeng Xue. Chemical bond analysis of the crystal growth of KDP and ADP. J. Cryst. Growth. 2006;286:108-113.
14. Dongli Xu, Dongfeng Xue. Chemical bond simulation of KADP single-crystal growth. J. Cryst. Growth. 2008;310:1385-1390.
15. Kzauo. Nakamoto. IR and Raman Spectra of Inorganic Co-ordination Compounds, Wiley & Sons, New York. 1986;168.
16. Silverstein RM, Clayton Basseler G, Morrill TC. Spectrometric Identification of Organic Compounds. V Edn, John Wiley & Hall: London; 1975.
17. Aripnammal S, Chandrasekaran S. Sanjeeviraja C. Low temperature photoluminescence studies on semiorganic tris thiourea copper (I) chloride single crystal. Cryst. Res. Technol. 2012;47:145-150.
18. Sankar R, Raghavan CM, Balaji M, Mohan kumar R, Jeyavel. Synthesis and Growth of Triaquaglycinesulfatozinc(II),  $[Zn(SO_4)(C_2H_5NO_2)(H_2O)_3]$ , a New Semiorganic Nonlinear Optical Crystal. R. Cryst. Growth & Design. 2007;7:348-355.
19. Vijayan N, Ramesh Babu R, Gunasekaran M, Gopalakrishnan R, Ramasamy P, Kumaresan R, Lan CW. Studies on the growth and characterization of p-hydroxyacetophenone single crystals. J.Cryst. Growth. 2003;249:309-315.
20. Robert R, Justin Raj C, Krishnan S, Jerome Das S. Optical and mechanical studies on unidirectional grown tri-nitrophenol methyl p-hydroxybenzoate bulk single crystal. Physica B. 2010;405:4274-4278.
21. Moore S, Stein WH. Methods in Enzymol. Academic Press: New York; 1948.
22. Misra PS, Mertz ET, Glover DV. Studies on Corn Proteins. VIII. Free Amino Acid Content of Opaque-2 Double Mutants. Cereal Chem. 1975;52:844-848.
23. Gopalan R, Subramanian PS, Rengarajan K. Elements of Analytical Chemistry. Sultan Chand & Sons: New Delhi; 2003.
24. Vijayabhaskaran B, Ramachandra Raja C. Influence of metallic substitution on the physical properties of nickel mercury thiocyanate nonlinear optical crystal. Optik. 2013;124:1366-1368.
25. Anie Roshan S, Cyriac Joseph, Ittyachen MA. Growth and characterization of a new metal-organic crystal: potassium thiourea bromide. Mat. Lett. 2001;49:299-304.
26. Kurtz SK, Perry TT. A Powder Technique for the Evaluation of Nonlinear Optical Materials. J. Appl. Phys. 1968;39:3798-3813.
27. Bhagavannarayana G, Kushwaha SK. Enhancement of SHG efficiency by urea doping in ZTS single crystals and its correlation with crystalline perfection as revealed by Kurtz powder and high-resolution X-ray diffraction methods. J. Appl.Cryst. 2010;43:154-162.

© 2013 Manimekalai and Raja; This is an Open Access article distributed under the terms of the Creative Commons Attribution License (<http://creativecommons.org/licenses/by/3.0>), which permits unrestricted use, distribution, and reproduction in any medium, provided the original work is properly cited.

Peer-review history:

The peer review history for this paper can be accessed here:  
<http://www.sciencedomain.org/review-history.php?iid=245&id=7&aid=1855>